SMiRT-12 / K. Kussmaul (Editor)
1993 Elsevier Science Publishers B.V.

GF01/5

CALCULATED WARM PRESTRESS AND SHALLOW CRACK EFFECTS IN A PTS-TRANSIENT

P. Rajamäki

IVO International Ltd., Finland

ABSTRACT

The effect of crack tip element size on J-integrals in a PTS transient was studied by performing finite element calculations with various sizes of crack tip elements, ranging from 0.004 mm to 0.548 mm. The calculation results indicate that the size of the tip element has a strong effect on the results during the interval of decreasing loading with diminishing J-integrals.

The shallow crack effect was studied by comparing the pressure vessel calculations with the calculations for a three-point bending specimen with a deep crack. The J-integrals of the three-point bending specimen were about 10-20% lower at the same level of crack opening mode stress than those of the pressure vessel model.

1 INTRODUCTION

The deterministic fracture mechanics calculations for the Loviisa 1 reactor pressure vessel (RPV) have been performed using various sizes of postulated sub-surface and surface cracks in the finite element models. In case of shallow and short surface cracks the most critical time interval existed during the latter half of the studied PTS transients. This interval of decreasing loading was examined more fully with axisymmetric finite element models using extremely small crack tip elements 0.004 - 0.05 mm.

2 EVALUATION OF WARM PRESTRESS EFFECT

The WPS effect was evaluated on the basis of the calculated J^*-integrals using in the axisymmetric models the crack tip element size of 0.004 mm and performing comparative calculations with the size of 0.548 mm, which was the actual size of the crack tip elements in the 3-D calculations for shallow and short surface cracks for the Loviisa 1 RPV.

J^*-integrals were calculated by the BERSAFE[1] finite element program. This J^*-integral is defined in BERSAFE as the limit of a

contour integral around the tip, as the size of the contour tends to zero. The J*-integral is a measure of the cohesive forces at the crack tip.

3 EVALUATION OF SHALLOW CRACK EFFECT

The effect of crack depth on unstable fracture was evaluated on the basis of the tensile stress on the crack plane[2]. The J-integrals from the RPV calculations were compared with the calculations of the three-point bending specimen (3-PB) when the crack opening mode stress was the same in both models. These stresses were compared at the distance[2] of 4 x CTOD (= 4 x crack tip opening displacement) ahead the crack tip.

4 NUMERICAL ANALYSIS

The analyses were performed using the BERSAFE finite element system[1]. Small strain theory and isotropic or kinematic hardening models were used. Cladding was taken into account in the RPV model. The stress-strain curves for base metal and for cladding are given in Table 1. The material properties of base metal (temperature-dependent) were used in the calculations of the three-point bending specimen.

Table 1. Stress-strain curves for calculations.

Base metal

	Equivalent Plastic strain	0.	0.0033	0.0087
Temp °C	Equivalent Stress (MPa)			
20		625.	695.	740.
325	-"-	555.	625.	670.

Cladding

	Equivalent Plastic strain	0.	0.25
Temp °C	Equivalent Stress (MPa)		
23		426.	645.
130	-"-	360.	520.
325.	-"-	326.	495.

The stress-free temperature of the RPV model was 230°C. The difference between the thermal expansion coefficients of cladding (16.3 - 17.4 x 10^{-6}) and the base metal (11.3 - 13.1 x 10^{-6}) produced a residual stress equal to 300 MPa in claddig at 20°C.

5 THE 10 mm DEEP SURFACE CRACK AND ISOTROPIC HARDENING

The pressure load was first raised to 13.7 MPa after which the thermal transient (Fig. 1) started. The pressure was constant during the transient. All the J*-integrals of seven paths (Fig. 2) are presented in Fig. 3. The surface integral between the integration path and the elements immediately around the crack tip were added to the line integral (*, *G= g-function method).

The crack tip elements are highly distorted at 1980 s (Fig. 5). These distortions may be the reason for the oscillations (Fig. 6) of the tensile stress at 1980 s. This oscillation existed at a distance of 0 -0.01 mm from the crack tip. The critical distance, 4 x CTOD, is at 1140 s equal to 0.06 mm and at 1980 s equal to 0.07 mm. Because of high element distortions, the results of the integration paths 1 and 2 were rejected, and the results from the paths 3 - 7 were compared with the calculations performed with the crack tip element size of 0.548 mm (Fig. 4).

The crack tip temperature of the RPV model is at 1140 s equal to 163.6°C. The shallow crack effect was studied by loading the 3-PB model (Fig. 7) at 163.6°C (uniform temperature) so that the tensile stress at 4 X CTOD is the same as in the RPV model at 1140 s. Same principles were applied to study the time point 1980 s. The shallow crack effect is indicated by the J-integrals in the 3-PB model, which are lower than in the RPV model (Fig. 8).

6 THE 15 mm DEEP SURFACE CRACK AND ISOTROPIC HARDENING

The same transient was calculated by two alternative pressure histories, with a constant pressure of 13.7 MPa or with a pressure rise from 4 MPa to 13.7 MPa at 2490 s (Fig. 9). In case of the pressure rise at the end of the transient the beneficial effects from warm prestress and shallow crack geometry seem to disappear.

7 THE 15 mm DEEP SURFACE CRACK AND KINEMATIC STRAIN HARDENING

The kinematic hardening model was used both in the RPV model (Fig. 10) and in the 3-PB model. A sublayer model for kinematic hardening and somewhat looser iteration tolerances than in the isotropic case were used. The tolerances were, however, the same for the RPV model and for the 3-PB model.

Only the case of pressure rise at 2490 s was studied (Fig. 11). According to these calculations there is a small beneficial shallow crack effect also in case of late pressure rise (Fig. 12).

8 CONCLUSIONS

According to these calculations made for one PTS transient, the effects of warm prestress and shallow crack geometry strongly depend on the pressure history of the transient.

So far neither the warm prestress effect nor the shallow crack

effect have been taken into account in the fracture mechanics calculations of the Loviisa reactor pressure vessels and further studies are needed before these effects can be considered.

REFERENCES

(1) BERSAFE user's manual. Level 6 Volume 3 BERSAFE non-linear. Nuclear Electric plc.
Berkeley Nuclear Laboratories, Berkeley England.

(2) Dodds R. H., Anderson T. L. and Kirk M. T.. 1991. A framework to correlate a/W ratio effects on elastic-plastic fracture toughness (J_c). International Journal of Fracture 48: 1-22.

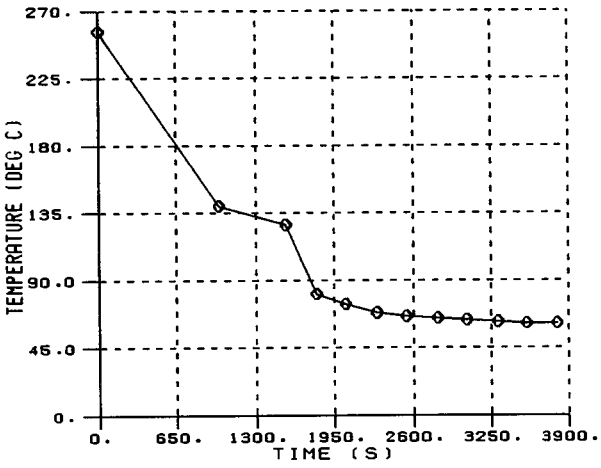

FIG. 1 TEMPERATURE HISTORY OF THE PTS TRANSIENT.

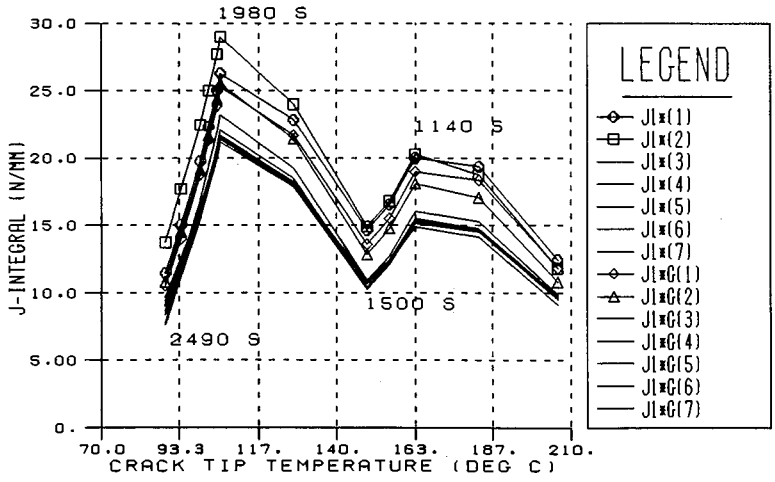

FIG. 3 J-INTEGRALS FOR THE PTS TRANSIENT.

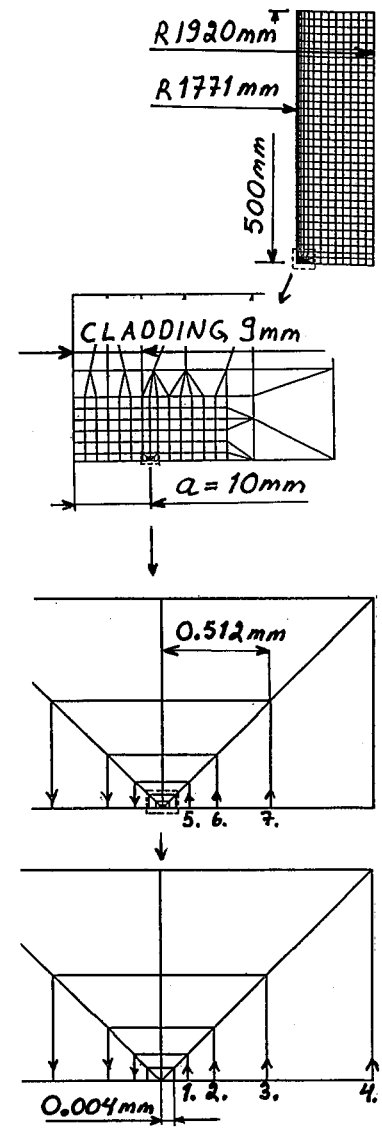

FIG. 2 FINITE ELEMENT MESH FOR 10 mm DEEP AND AXISYMMETRIC SURFACE CRACK.

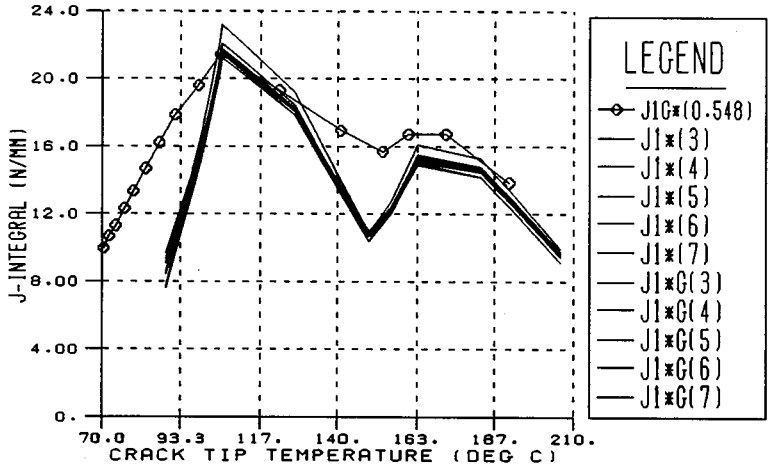

FIG. 4 COMPARISON OF J-INTEGRALS FOR CRACK TIP ELEMENT SIZES OF 0.548 mm AND 0.004 mm.

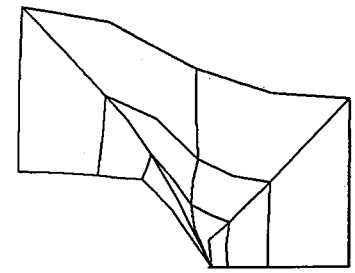

FIG. 5 CRACK TIP DEFORMATIONS IN SCALE 1:1 (DEFORMATIONS:GEOMETRY).

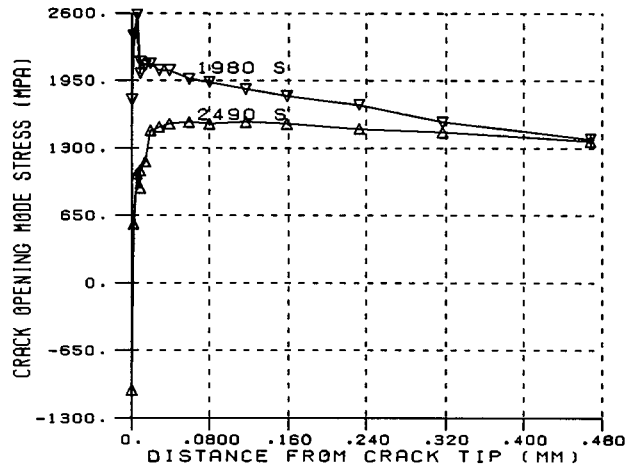

FIG. 6 OPENING MODE STRESSES NORMAL TO THE CRACK PLANE.

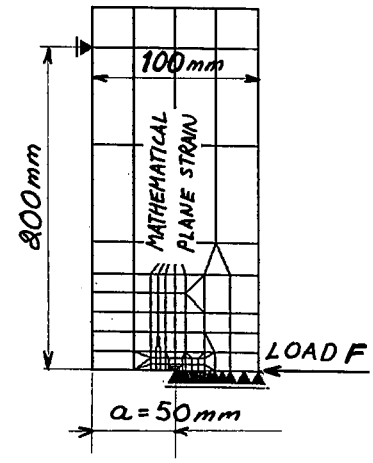

FIG. 7 FINITE ELEMENT MESH FOR THREE POINT BENDING SPECIMEN (3-PB).

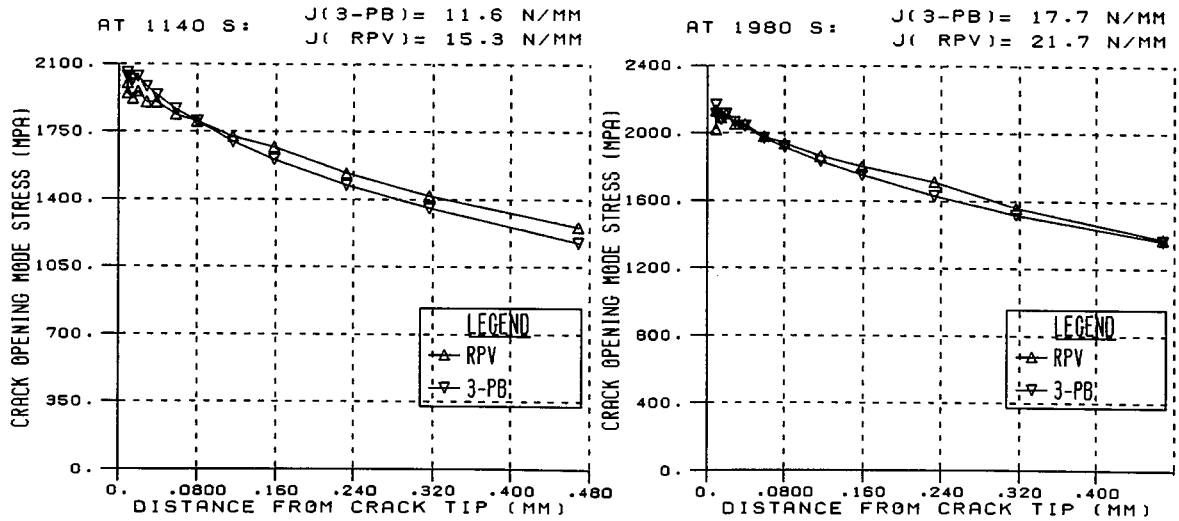

FIG. 8 COMPARISON OF CRACK OPENING MODE STRESSES IN RPV AND 3-PB SPECIMEN.

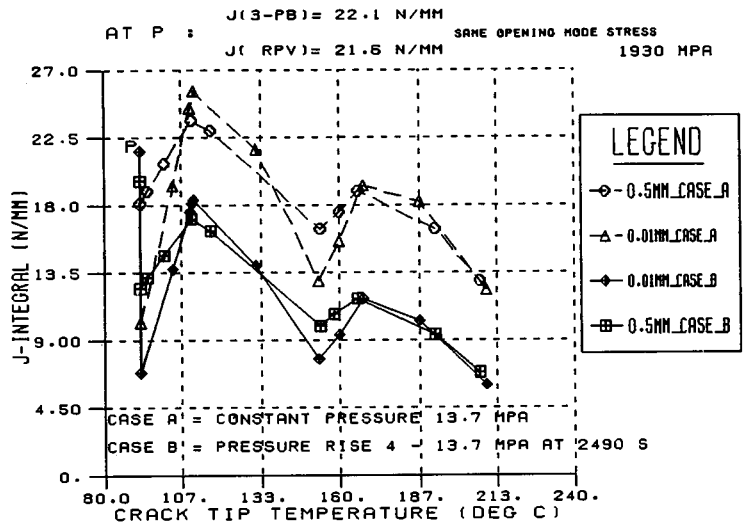

FIG. 9 COMPARISON OF J-INTEGRALS FOR CRACK TIP ELEMENT SIZES OF 0.01 mm AND 0.5 mm.

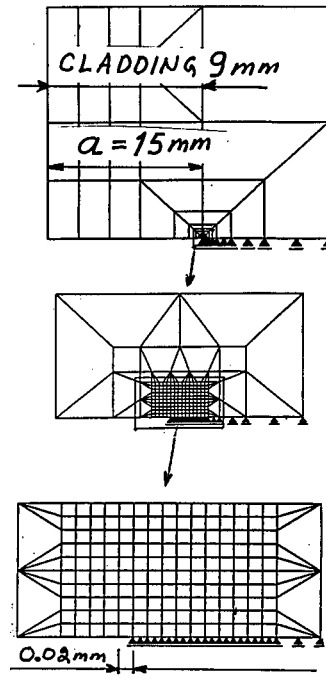

FIG. 10 FINITE ELEMENT MESH FOR 15 mm DEEP AND AXISYMMETRIC SURFACE CRACK.

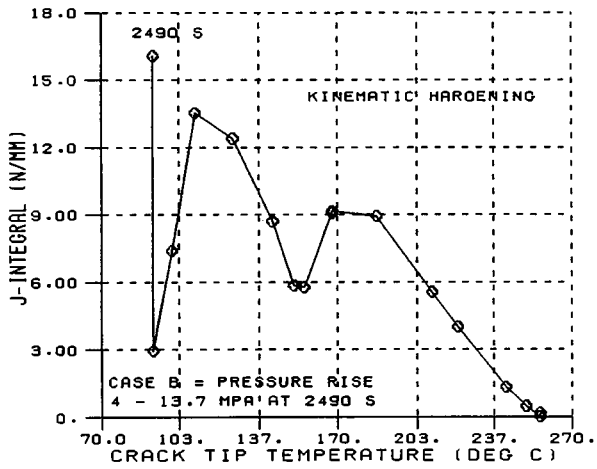

FIG. 11 J-INTEGRALS IN CASE OF KINEMATIC MATERIAL HARDENING.

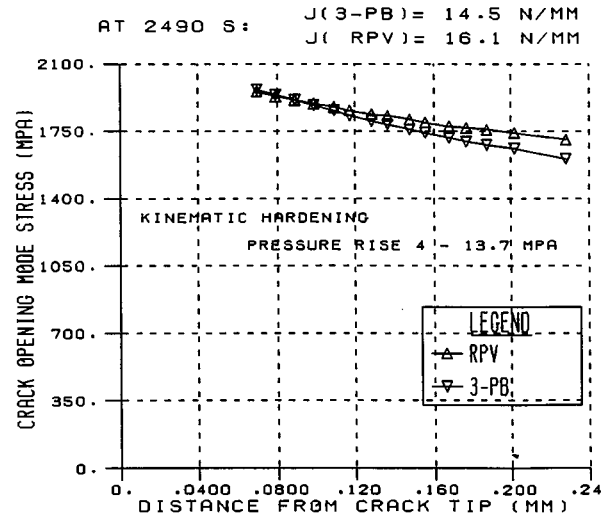

FIG. 12 COMPARISON OF CRACK OPENING MODE STRESSES IN RPV AND 3-PB MODELS IN CASE OF KINEMATIC MATERIAL HARDENING.